Wegener Center for Climate and Global Change
University of Graz
Leechgasse 25, A-8010 Graz, Austria

Atmospheric Remote Sensing and Climate System Research Group

WegCenter/UniGraz Technical Report for FFG-ALR No. 1/2007

FFG-ALR study:

ACCURAID – Aid to ACCURATE Climate Satellite Mission Preparations

[Contract No: ALR-OEWP-WV-327/06 – January 2007]

ENHANCEMENT REPORT

[WP2: ENHANCE]

Enhancement of the end-to-end occultation simulation tool EGOPS for enabling quasi-realistic simulations of LEO-LEO IR laser occultation measurements

S. Schweitzer, G. Kirchengast, and F. Ladstädter

Wegener Center for Climate and Global Change (WegCenter),
University of Graz, Graz, Austria

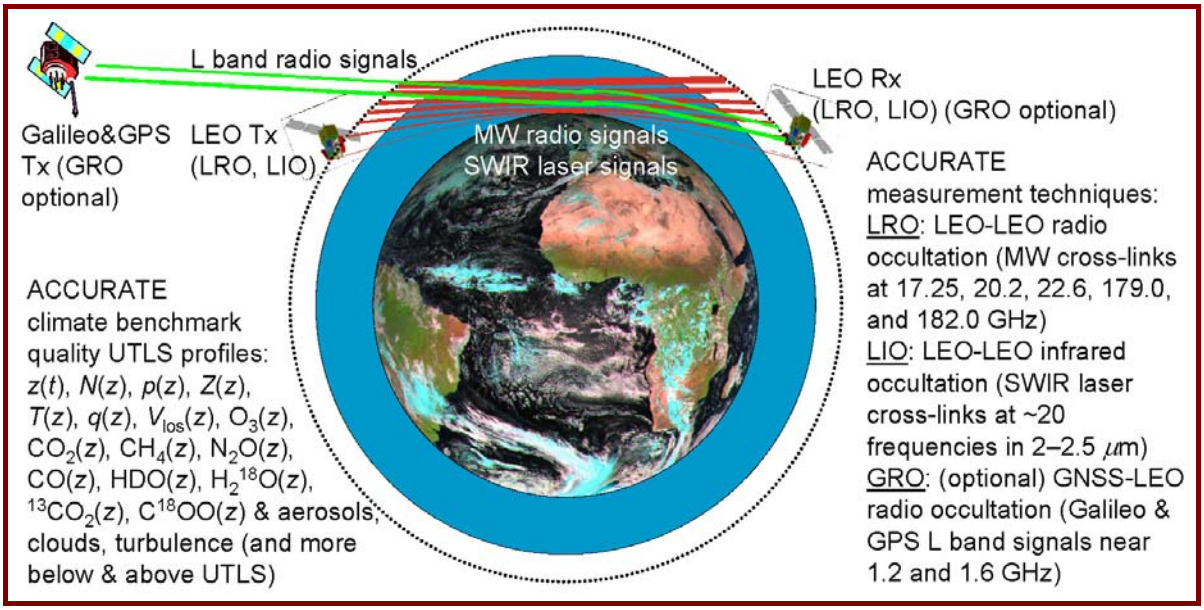

April 2007

(intentionally left blank; back page if double-sided print)

Table of Contents

(intentionally left blank; back page if double-sided print)

List of Acronyms

ACCURATE	Atmospheric Climate and Chemistry in the UTLS Region and Climate Trends Explorer
ACE+	Atmosphere and Climate Explorer mission (ESA mission concept 2002–2004)
CH_4	Methane
$C^{18}OO$	Carbon dioxide isotope (with one heavy-oxygen atom ^{18}O)
CO	Carbon monoxide
$^{13}CO_2$	Carbon dioxide isotope (with one heavy carbon atom ^{13}C)
CO_2	Carbon dioxide
ECMWF	European Centre for Medium-Range Weather Forecasts (Reading, U.K.)
EGOPS5	End-to-end Generic Occultation Performance Simulator, Version 5
Envisat	Environmental Satellite (of the European Space Agency)
EOPSCLIM	End-to-end Occultation Processing System: MetOp GRAS-IASI and ACCURATE Integration (FFG-ALR study)
ESA	European Space Agency
ESA-Prodex	An ESA Programme line (for an enlisted subgroup of member states, incl. Austria)
ESRL	Earth System Research Laboratory, NOAA institution
FASCODE	FASt Atmospheric Signature CODE
FFG-ALR	Österr. Forschungsförderungsgesellschaft–Agentur für Luft- und Raumfahrt
FoMod	Forward Modeling System, subsystem of EGOPS
GALILEO	European future global navigation satellite system
GCM	Global Circulation Model
GHGs	Greenhouse Gases
GNSS	Global Navigation Satellite Systems (Global Positioning System GPS, and Galileo)
GOMOS	Global Ozone Monitoring by Occultation of Stars (Envisat stellar occ. instrument)
GPS	Global Positioning System
GRO	GNSS-LEO Radio Occultation (here Galileo & GPS L band signals, ~1.2 / 1.6 GHz)
H_2O	Water vapour
$H_2{}^{18}O$	Water vapour isotope (with one heavy-oxygen atom ^{18}O)
HDO	Water vapour isotope (with one heavy-hydrogen=deuterium atom)
HITRAN	High-resolution Transmission molecular absorption database
InRet	Inversion/Retrieval, subsystem of EGOPS
LEO	Low Earth Orbit
LIO	LEO-LEO Infrared Occultation (here laser cross-link signals within 2–2.5 μm)
LOWTRAN	Low Resolution Transmission (Model)
LRO	LEO-LEO Radio Occultation (here cross-link signals within 17–23 and 178-183 GHz)
MAnPl	Mission Analysis Planning System, subsystem of EGOPS
MW	Microwave spectral region
N_2O	Nitrous oxide
NEP	Noise Equivalent Power
NOAA	U.S. National Oceanic & Atmospheric Administration
O_3	Ozone
OSMod	Observation System Modeling, subsystem of EGOPS
RFM	Reference Forward Model
Rx	Receiver satellite
SWIR	Short wave infrared spectral region (1.5-3 μm; here referring to the 2–2.5 μm region)
Tx	Transmitter satellite
UniGraz	University of Graz (Austria)
UTLS	Upper Troposphere/Lower Stratosphere height region
WP	Work Package

List of Symbols

α_M	Molecular absorption coefficient
α_t	Full angle of the Gaussian laser beam divergence (at e^{-2} radius points)
ε_A	Aerosol extinction coefficient
λ	Wavelength
σ_R	Rayleigh scattering coefficient
$\sigma_{I,th}$	Thermal noise standard error
a	Ångstrøm exponent
A_r	Receiving optics reception area (reception mirror/telescope area)
d_r	Diameter of the circular receiver optics
D_{tr}	Distance between transmitter and receiver
e	Water vapour pressure
f_s	Sampling rate
I, I_0	Intensity, unattenuated intensity
L_{atm}	Loss due to atmospheric attenuation
L_{opt}	Total optical loss of the receiver
L_{rec}	Reception loss of the receiver (due to integration time > laser pulse period)
L_{tr}	Signal propagation loss (in free space)
N	Refractivity
N_{air}	Number density of air
n	Index of refraction
NEP_r	Noise-Equivalent Power (of the optical detectors in the receiving system)
P_t, P_r	Transmitted and received power, respectively
p	Pressure (total air pressure)
s	Ray path coordinate
S/N_0	Signal-to-noise density ratio [dBHz] (at 1 Hz unit bandwidth)
SNR	Signal-to-noise ratio [dB] (generic)
SNR_{fs}	signal-to-noise ratio at the simulated sampling rate f_s [dB]
T	Temperature
V_{los}	Line-of-sight wind velocity
w_r	Radius of the Gaussian laser beam (e^{-2} radius) at the receiver
z	Height over Earth's surface

1 Background and Context

1.1 The ACCURATE Mission

ACCURATE is a next generation climate mission which employs the occultation measurement principle, known for its unique combination of vertical resolution, accuracy, and long-term stability, in a novel way (for background information on the utility of occultations in climate sciences see *OPAC*, 2004a). It systematically combines use of highly stable signals in the MW 17-23/178-183 GHz bands (LEO-LEO radio crosslink occultation, LRO) with laser signals in the SWIR 2–2.5 μm band (LEO-LEO infrared laser crosslink occultation, LIO) for exploring and monitoring climate and chemistry in the atmosphere with focus on the Upper Troposphere/Lower Stratosphere region (UTLS, 5–35 km). The MW radio occultation is an advanced and at the same time compact version of the LEO-LEO MW radio occultation concept studied in 2002-2004 for the ACE+ mission project of ESA for frequencies including the 17-23 GHz band (*ESA* 2004a,b; *OPAC* 2004b), complemented by U.S. study heritage for frequencies including the 178-183 GHz band (e.g., *Kursinski et al.*, 2002). The core of ACCURATE is tight synergy of the SWIR laser crosslinks with the MW radio crosslinks. Concerning laser-based sounding technologies, strong heritage exists from Envisat and Earth Explorer activities. Optionally also a Galileo/GPS component (GNSS-LEO occultation, GRO) is planned in order to demonstrate the use of Galileo-LEO radio occultation.

The ACCURATE mission concept was conceived at the Wegener Center/Uni Graz in late 2004 and proposed in 2005 (*ACCURATE*, 2005) by an international team of more than 20 scientific partners from more than 12 countries to an ESA selection process for next Earth Explorer Missions (*ESA*, 2005). In a stringent scientific and technical peer assessment process, it received very positive evaluation and recommendations for further study (*ESA*, 2006). It was acknowledged that ACCURATE can act as a cornerstone contribution to the priority "Atmospheric Chemistry and Climate" of the "Priorities for 2005 Call" (section 6 in *ESA*, 2005) and also provides vital contributions related to the atmospheric subsystem of the Earth system for the priorities "The Global Water Cycle" and "The Global Carbon Cycle".

The concept for the ACCURATE mission is drawn from the best features learned so far in the occultation field on signal source, atmospheric signal propagation and radiation-atmosphere interaction, receiving system properties, and data processing methodologies. ACCURATE is set out to initiate and establish an unprecedented global data set of profiling the atmospheric physical, chemical, and climatic state over the UTLS domain at high vertical resolution, accuracy, and long-term stability. Due to their unique utility for climate trends monitoring and climate model validation and improvement based on their un-biased nature, these data are also termed climate benchmark data.

The observed parameters are measured simultaneously and in a self-calibrated manner based on Doppler shift and differential log-transmission profiles. In particular, the fundamental thermodynamic variables of the atmosphere (temperature, pressure/geopotential height, humidity) are retrieved from the MW bands, complemented by line-of-sight wind, six greenhouse gases (GHGs) and key species of UTLS chemistry (H_2O, CO_2, CH_4, N_2O, O_3, CO) and four water vapour and carbon isotopes (HDO, $H_2{}^{18}O$, $^{13}CO_2$, $C^{18}OO$), which are retrieved from the SWIR band. Furthermore, profiles of aerosols, cloud layering, and turbulence are

obtained, mainly based on direct (single-channel, non-differenced) transmission profiles. All profiles come with accurate height knowledge (< 10 m uncertainty), since measuring height as a function of time is intrinsic to the LRO part of the ACCURATE observing system.

1.2 The Contribution of ACCURAID

The overall purpose of the ACCURAID project is an initial assessment of the scientific utility and performance of the novel LEO-LEO infrared occultation (LIO) part of the ACCURATE mission concept. With regard to the GRO and LRO parts, no work is done within this project because measurement process and data retrieval performance of these parts have been studied to some detail in previous work and are continued elsewhere.

ACCURAID is a preparatory and accompanying study in the context of the ACCURATE mission development. In particular, two main goals are pursued in two work packages (WP 1 is Project Management):

WP 2 – Enhancement of an existing end-to-end radio occultation simulation tool (EGOPS) for enabling quasi-realistic simulations of LIO measurements,
WP 3 – Initial end-to-end analysis of retrieval performance for greenhouse gas and isotope profile retrievals from LIO data.

The work on WP 2 is based on further advancement of the End-to-end Generic Occultation Performance Simulator Version 5 (EGOPS5; *Kirchengast et al*., 2004b; 2007), an internationally leading occultation simulator having meanwhile involved more than 10 years of development by international scientific teams led by Univ. of Graz. This scientific simulation tool enables end-to-end simulation of GRO and LRO measurements. In order to enable the simulation of LIO occultation measurements, too, the forward and observation system modelling part, which simulates the influence of the Earth's atmosphere and of the instrumental properties on the propagating electromagnetic signals, is enhanced for infrared laser cross-links. One main task is the implementation of a so-called "full atmosphere model", which enables inclusion of profiles/fields of greenhouse gases, isotope species, and wind beyond the existing LRO variables refractivity, pressure, temperature, and humidity. A second one is the development of a module for seamlessly computing absorption coefficients of all relevant gases at arbitrary infrared frequencies, and the third main task is the simulation of atmospheric effects influencing the propagating SWIR signals, as well as the simulation of modifications of SWIR signals due to instrumental errors.

The work on WP 3 is carried out on the basis of a simplified EGOPS-external LIO end-to-end performance estimation chain, the ALPS (ACCURATE LIO Performance Simulator) system (*ACCURAID*, 2007), which is obtaining simulated measurements from the RFM forward modelling system (*RFM*, 1996 & 2007). The main objective of WP 3 is an initial assessment of the retrieval performance of H_2O and its isotopes, of CO_2 and its isotopes, and of the other greenhouse gases N_2O, CH_4, O_3, and CO. In addition, performance of the line-of-sight wind (V_{los}) retrieval is assessed. This enables to estimate the potential utility of LIO data for atmosphere and climate science.

Altogether, ACCURAID is an important supporting element to the development of ACCURATE and the novel LIO method, and is therefore one fundamental step for an implementation of this mission in the future.

2 Enhancement of the EGOPS5 Software by Essential LIO Capabilities

This chapter comprises the description of the activities, which have been done within the scope of WP 2 of ACCURAID. The enhancement of EGOPS (End-to-end Generic Occultation Performance Simulator) was concentrated on the extension of the Forward Modeling (FoMod) and Observation System Modeling (OSMod) part of the software in order to enable quasi-realistic simulation of the propagation of SWIR (short wave infrared) laser signals through the atmosphere as well as of the reception of the signals at the receiver. In the course of the work, the strong requirement emerged that the atmospheric models system, a subcomponent of the FoMod system, needs significant restructuring and that the LIO requirements for seamless inclusion of profiles/fields of greenhouse gases, isotope species, and wind – beyond the existing LRO variables refractivity, pressure, temperature, and humidity – demand a new type of "full atmosphere model". In addition, the algorithm development for seamlessly computing absorption coefficients of all relevant gases at arbitrary infrared frequencies, integrating the Reference Forward Model (*RFM*, 1996 & 2007), which in turn uses the HITRAN 2004 molecular spectroscopic databases (*Rothman et al.*, 2005; *HITRAN*, 2007), was a demanding challenge. Regarding inversion/retrieval, an initial EGOPS-external simulation system (the ACCURATE LIO Performance Simulator, ALPS) was developed, for the scientific retrieval performance analyses under WP 3 (*ACCURAID*, 2007).

In the following, a brief description of the EGOPS5 software will be given (section 2.1) in order to facilitate the comprehension of the EGOPS enhancements characterized afterwards (section 2.2).

2.1 The Simulation Tool EGOPS5

The End-to-end Generic Occultation Performance Simulator, Version 5, is a software package allowing the end-to-end simulation of GRO and LRO measurements. Its main purpose is to support research addressing scientific and mission analysis questions on the GNSS-LEO/LEO-LEO based radio occultation technique. It is composed of a series of modules, which are integrated into so-called Systems (see Fig. 1). The Mission Analysis and Planning (MAnPl) System allows analysis and planning of GNSS-LEO and LEO-LEO satellite constellations with regard to their suitability for occultation missions. In particular, its main capability is that the distribution of occultation events around the globe can be simulated using arbitrary (user-generated) satellite constellations. Based on the resulting geometry data of such occultation events, the Forward Modeling (FoMod) System together with the Observation System Modeling (OSMod) System enables quasi-realistic simulation of GNSS-LEO as well as LEO-LEO radio occultation observables (i.e., phase and amplitude profiles at each signal frequency) and related required variables. In particular, FoMod's task is to simulate the electromagnetic signal propagation through the atmosphere (and ionosphere) towards the receiver based on orbital motions of transmitter and receiver satellites. The resulting occultation signals are influenced by atmospheric (and ionospheric) effects. Effects due to the receiving system (instrumental errors, in general), which usually perturb the signal quality, are superimposed during the subsequent OSMod simulation. Finally, the Inversion/Retrieval (InRet) Sys-

tem is responsible for the retrieval processing of simulated or observed GRO/LRO phase and amplitude data (supplemented by the necessary geometry information) in order to obtain quasi-vertical profiles of atmospheric parameters. The retrieval algorithms for GRO and LRO differ somewhat: In the case of LRO, phase and amplitude data are converted via bending angles and transmissions down to profiles of refractivity and absorption coefficients, density, pressure (or geopotential height), temperature, and humidity (as well as liquid water if needed). In the case of GRO, only bending angles are exploited, which is why no frequency-dependent absorption coefficients can be utilized to independently retrieve humidity. A more detailed overview of the scientific retrieval algorithms for both GRO and LRO data processing is given by *Kirchengast et al.* (2004a).

The four systems mentioned above are the core of EGOPS5. Additionally, there is a so-called Visualization/Validation System, which enables post-processing of the retrieved data (statistics, visualization, etc.), including the capability to extract information from the atmosphere system underlying the occultation simulations. Altogether, EGOPS5 enables research contributing to a better quantification of the potential of the GRO and LRO occultation technique for atmosphere and climate science.

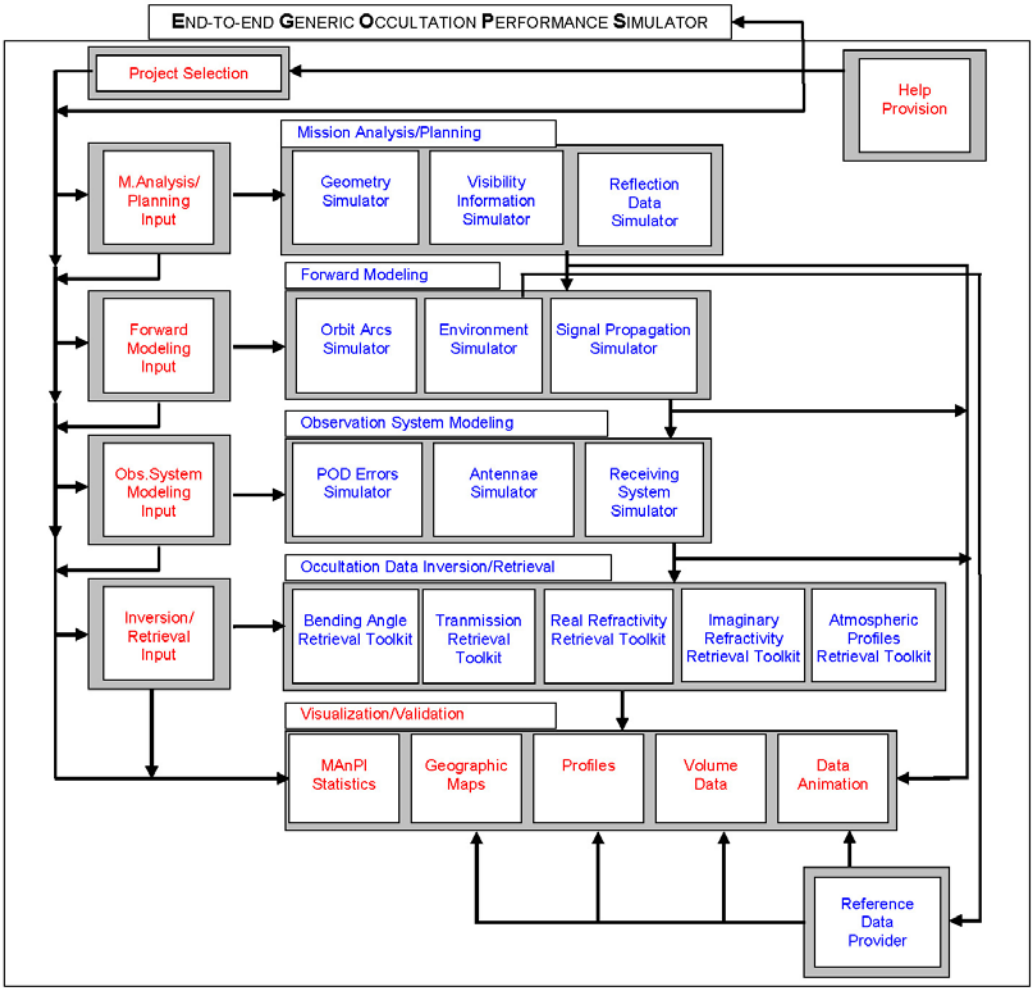

Fig. 1: Modular view of EGOPS5 (from *Kirchengast et al.*, 2007).

2.2 EGOPS Enhancement

The implementation of the capability to model quasi-realistic LIO measurements in the ACCURAID project concerned the FoMod and the OSMod part of EGOPS. In the following, the tasks which were performed regarding the scientific-technical algorithm development will be described separately for each of these parts.

2.2.1 Enhancement of the FoMod System

In general, three main tasks were executed concerning the extension of the FoMod System. First, a so-called "full atmosphere model" was implemented, which allows to get the full atmospheric state including vertical profiles of refractivity, pressure, temperature, humidity, greenhouse- and trace gas concentrations, and horizontal wind velocity at arbitrary geographic locations. Second, the Reference Forward Model (*RFM*, 1996 & 2007), which enables to compute absorption coefficients on the basis of the HITRAN molecular absorption database (*Rothman et al*., 2005; *HITRAN*, 2007) and the FASCODE atmospheres (*Anderson et al.*, 1986) made accessible via the "full atmosphere model", was incorporated into the EGOPS system for absorption coefficient simulations. Third and last, simple models for various atmospheric influences, which additionally attenuate and/or perturb the propagating laser signals, were included. These are defocusing loss, Rayleigh scattering, aerosol extinction, turbulence/scintillation loss, and the influence of wind velocity in line-of-sight direction, respectively.

The full atmosphere model

Since the purpose of the LIO laser links is to enable the measurement of the abundance of different atmospheric gases, the frequency of an individual signal is lying in the centre of an absorption line of a specific gas, where the absorption of other gases is comparatively low. This is why each signal is mainly absorbed by one atmospheric constituent and this, in turn, allows to retrieve the concentration of that constituent from measurements of the transmission of the signal (in combination with the bending of the signal, which is determined from simultaneous LRO measurements). An overview of this retrieval principle is shown in Fig. 2. Forward modelling of atmospheres and absorption coefficients is a basis for this analysis.

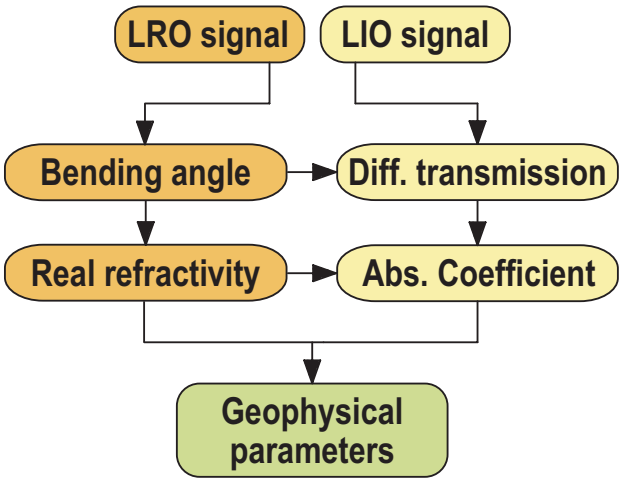

Fig. 2: Simplified overview of a LIO retrieval processing chain based on the differential transmission principle.

Because the FoMod part of EGOPS did not work with atmospheric trace gases so far, it was needed to integrate an atmospheric model, which delivers the concentration of the absorbing gases. Initially, a set of six atmospheric states (tropical, mid-latitude summer/winter, subarctic summer/winter; U.S. standard) obtained from the well-known FASCODE software package is used for this purpose. Since the atmosphere models existing so far in EGOPS are for the thermodynamic parameters (refractivity, temperature, humidity), the involvement of the trace gases would have been too complex. This is why the need for restructuring of the atmospheric models system of FoMod arose, which entailed the development of the so-called "full atmosphere model".

The full atmosphere model is a thoroughly newly developed module for atmospheric model data to provide the trace gas concentrations along with the common atmospheric parameters such as temperature, pressure, and refractivity. Its implementation happened with extensibility in mind, by effectively decoupling the interface for providing atmospheric data from the underlying file-based atmospheric profiles or field data. It is aimed at later replacing the existing atmospheric models in EGOPS, providing always the same clear interface. The full atmosphere model, currently for 1D vertical profiles (FASCODE and U.S. standard atmospheres), is flexible and prepared to be extended when needed by, e.g., 2D and 3D models. Furthermore, combination of atmospheric data from different models is possible.

In order to guarantee full consistency between all atmospheric parameters, the full atmosphere model is able to use a "refractivity based" mode, where the refractivity N is the basic parameter, from which pressure and temperature is derived. This emulates the mode of previous EGOPS atmosphere models. Thereby, depending on the frequency of the signal, the appropriate formula is used to calculate the refractivity first out of the gridded temperature, pressure and humidity data. This is then the basic parameter used for the high-accuracy ray tracer in order to compute the ray path, as well as for the modelling of consistent atmospheric data via numerical integration of the barometric formula and use of the equation of state, in analogy to the atmospheric profiles retrieval process in radio occultation data processing (e.g., *Kursinski et al.*, 1997).

The full atmosphere model automatically deduces, from the respective frequency used, which refractivity formula must be applied in order to ensure correct handling of the signal. In the case of SWIR signals, the Edlen Formula is employed (*Edlen*, 1966),

$$N(z) = \frac{0.28438[\mathrm{K/hPa}]}{1.00062} \cdot \left(83.4213 + \frac{24060.3}{130 - \frac{10^6}{\lambda[\mathrm{nm}]^2}} + \frac{159.97}{38.9 - \frac{10^6}{\lambda[\mathrm{nm}]^2}} \right) \cdot \frac{p(z)[\mathrm{hPa}]}{T(z)[\mathrm{K}]}, \qquad (1)$$

where N is the refractivity, λ is the wavelength of the signal, p is (total air) pressure, T is temperature, and z is the height. For the MW spectral range, the Smith-Weintraub Formula is utilized (*Smith and Weintraub*, 1953),

$$N(z) = 77.60 \cdot \frac{p(z)[\mathrm{hPa}]}{T(z)[\mathrm{K}]} + 3.73 \cdot 10^5 \cdot \frac{e(z)[\mathrm{hPa}]}{T(z)[\mathrm{K}]^2}. \qquad (2)$$

Currently, the full atmosphere model supports FASCODE atmospheres as well as GCM-derived vertical profiles of wind (zonal and meridional components), because these models were used for the demonstration of the functionality of the LIO forward modelling system (see chapter 3). In the future, all existing, and if needed also other new models, can be integrated into the full atmosphere model, which will be done in the future as resources permit.

Integration of the Reference Forward Model RFM

The computation of the transmission of SWIR signals needs knowledge on the abundance of absorbing gases as well as on their absorption coefficients, which depend among other things on temperature and pressure. Originally (ACCURAID proposal) it was planned to compute the absorption coefficients from the HITRAN 2004 high-resolution transmission molecular absorption database (distributed by the Harvard-Smithsonian Center for Astrophysics, Cambridge, Massachusetts, USA) using the Reference Forward Model (RFM, leadingly developed by *A. Dudhia*, Univ. of Oxford, United Kingdom; http://www-atm.physics.ox.ac.uk/RFM) and to couple the output in the form of absorption coefficient table files into the software. But this turned out to be unacceptably inefficient, because a huge amount of different "lookup table" files of considerable size would have been needed in order to enable to compute the absorption coefficients of all contributing gases (about 20 in number) at arbitrary combinations of temperature and pressure. Therefore, it was decided to directly integrate the RFM model, at software code level, into the EGOPS system. Thus, the absorption coefficient can now be computed in an integrated manner at each point of signal propagation ray paths, based on local pressure and temperature at these points. This method is considerably more flexible and efficient than the method initially projected, though the CPU-demands for full-fledged forward modelling computations are still significant.

The integration of the RFM software package into the EGOPS system was very demanding, because as small as possible modifications within the software were desired so that also future versions of RFM can easily be integrated. This entails many advantages, because RFM is continually enhanced. Thus, a software interface was developed, which converts the RFM package, which must be obtained from the lead developer *A. Dudhia* (RFM is not distributed with EGOPS), into an EGOPS subroutine. This subroutine is compiled together with all other EGOPS routines and delivers the absorption coefficient of any gas at the desired temperature and pressure via a single subroutine. In the future, the interface will need either no or only small modifications if a new version of RFM is released, a factor decisive for the efficient maintainability of the system.

Modelling of atmospheric influences other than trace gas absorption on the signal

During the propagation of a ray through the atmosphere, it experiences miscellaneous impacts. In the case of SWIR signals, besides absorption due to trace gases also defocusing loss, Rayleigh scattering loss, aerosol extinction loss, and turbulence/scintillation loss play a role. Furthermore, wind in line-of sight direction of the ray influences the measurement, because absorbing molecules "see" a Doppler-shifted frequency, when they collectively move over large scales as they do in case of wind. In order to enable simulation of the ray propagation including these effects, simple models for each of these effects have been embedded into the FoMod system. In future more advanced models will be developed for some of these effects (e.g., aerosols, where under the ACCURAID successor project EOPSCLIM a significantly more realistic model is planned).

The absorption loss follows the Bouguer-Lambert-Beer law, which states that the attenuation of a signal, when passing an absorbing matter, is

$$I = I_0 \cdot e^{-\tau} = I_0 \cdot e^{-\int \alpha_M(s) ds}, \quad (3)$$

where I and I_0 are the intensity after and before absorption, respectively, τ is the optical thickness, α_M [m^{-1}] is the molecular absorption coefficient, and s [m] is the geometrical ray path followed by the signal through the absorbing matter. The LIO principle needs not to know the absolute intensity value, but the ratio I/I_0, which is the so-called transmission. Thus, the absorption loss within EGOPS is computed via numerical integration (Simpson's trapezoidal rule summation) of the product $\alpha_M \cdot ds$ within small sections ds along the ray path. Thereby, the information on the points along the ray path is coming from the EGOPS ray tracer and the absorption coefficient is computed using the RFM subroutine described above.

Concerning defocusing loss, no new models had to be involved because defocusing in the SWIR range follows the identical physics as defocusing in the MW range. Thus defocusing modeling was already included in the EGOPS high-accuracy ray tracer system from GRO/LRO developments. The only difference in application to LIO is that the actual ray path for SWIR and MW signals is slightly different, which demands the use of the adequate refractivity model in each case (the *Edlen* equation in case of SWIR signals, see Eq. (1), and the *Smith-Weintraub* equation in case of MW radio signals, see Eq. (2), respectively).

Rayleigh scattering is not affecting MW signals but is of interest for SWIR signals. The Rayleigh scattering loss can be computed according to Eq. (3) above, if the so-called Rayleigh scattering coefficient σ_R is used in addition to the absorption coefficient α_M. The model, which has been integrated into FoMod uses the following relation for computation of σ_R (after *Liou*, 2002),

$$\sigma_R[\mathrm{m}^{-1}] = \frac{32 \cdot \pi^3 \cdot (n-1)^2}{3 \cdot \lambda[\mathrm{m}]^4 \cdot N_{air}[\mathrm{m}^{-3}]}, \quad (4)$$

where $n = 1 + 10^{-6} \cdot N$ is the refractive index and N_{air} is the number density of air.

Regarding aerosol extinction and turbulence/scintillation loss, two very simple empirical models have been developed, which allow to roughly estimate the magnitude of their perturbation in the SWIR spectral range to an acceptable initial accuracy. More realistic models are certainly needed (and planned to be developed in ACCURAID successor projects) in the future. In the case of aerosol extinction loss, two profiles of mean aerosol extinction coefficients ε_A in "clear" and "volcanic" air (with severe stratospheric sulphate aerosol impact) at a wavelength of 500 nm were extracted from literature (LOWTRAN profiles, referring to a NOAA ESRL on-line report, *NOAA*, 2005). These extinction profiles can be selected as alternative cases and are scaled from 500 nm to any specific SWIR laser frequency of interest by an Ångstrøm law for the wavelength dependence of aerosol extinction,

$$\varepsilon_A[\mathrm{m}^{-1}] = \varepsilon_{A,\lambda 0}[\mathrm{m}^{-1}] \cdot \left(\frac{\lambda_0}{\lambda} \right)^a, \quad (5)$$

where ε_A and $\varepsilon_{A,\lambda 0}$ are the aerosol extinction coefficients at the desired wavelength λ and the reference wavelength λ_0 (in our case 500 nm), respectively, and a is the Ångstrøm exponent, which is assumed to be $a = 1.5$ (a conservative value for > 1 μm in the UTLS, may well be ~2 as well; cf. *Salby*, 1996; *Russell et al.*, 1996; *Thomason and Taha*, 2003). From this extinction profile, aerosol extinction loss is then computed according to Eq. (3), with ε_A used in addition to α_M (species absorption) and σ_R (Rayleigh scattering).

For the modelling of the turbulence/scintillation loss, two extinction coefficient profiles of scintillation loss [m^{-1}] – one is an upper limit/worst case estimate and the other one is just a test profile allowing to further artificially raise this loss – have been formulated at 500 nm from Envisat/GOMOS turbulence/scintillations experience and discussions with the experts *M. Gorbunov*, *V. Sofieva*, and *F. Dalaudier* (pers. communications, 2006). These are scaled to the SWIR wavelengths of interest via the same relation as embodied by Eq. (5). Also this extinction coefficient is added to the optical thickness integrand in Eq. (3).

As mentioned above, the effect of wind blowing in the direction of the laser beam propagation (V_{los}) was modelled, too. This is needed because molecules which collectively move in form of wind, absorb a slightly different frequency than molecules at rest in a motionless atmosphere (Doppler shift). This difference is non-negligible when using SWIR frequencies at the frequency accuracy and precision demanded by the ACCURATE LIO concept. The modelling of this effect required to implement the ability of extracting wind vector profiles from GCM-analyses into the full atmosphere model (we used ECMWF analyses, cf. section 3). Based on these wind vectors, V_{los} and the resulting Doppler frequency shift are then computed at each ray point via vector-analytical methods and, subsequently, absorption coefficients α_M are computed at correctly Doppler-shifted frequencies.

2.2.2 Enhancement of the OSMod System

Comparatively smaller adaptations than in FoMod where needed concerning the Observation System Modeling part of EGOPS, because the main sources of instrumental noise of the IR receiving system as designated for ACCURATE (ExtInGaAs detectors, etc.) are thermal noise and intensity drifts, which were already integrated in a similar manner in EGOPS5 for LRO simulations. Nevertheless, because the propagating signals in the case of LIO are laser intensity beams (rather than signal amplitudes in case of LRO), propagation loss and receiver noise must be modelled in a somewhat different way than for LRO signals.

The free-space propagation loss of SWIR laser signals from transmitter to receiver, L_{tr}, is defined by the ratio of the received power P_r to the transmitted power P_t, whereby no atmospheric attenuation effects are taken into account. It is determined by the dimension of the reception area A_r of the receiver front optics (reception mirror area) as well as by the beamwidth w_r of the 2D-Gaussian-shaped laser beam at the distance D_{tr} of the receiver from transmitter,

$$L_{tr} = \frac{P_r}{P_t} = \frac{2A_r}{w_r^2 \cdot \pi} \quad , \tag{6}$$

with

$$w_r = D_{tr} \cdot \frac{\alpha_t}{2}, \quad A_r = \frac{d_r^2}{4} \cdot \pi \ , \tag{7}$$

where w_r is derived from the product of D_{tr} and the laser beam divergence angle at the e^{-2} points of the Gaussian beam shape, α_t, and where the reception area A_r is modelled to simply derive from the diameter of a circular reception mirror, d_r.

In addition to this free-space loss L_{tr} also the reception loss, L_{rec}, from a receiver integration time longer than the signal pulse period, and the total optical loss, L_{opt}, from transmission losses in the optics of the receiving system from front-end reception mirror to the optical detectors, were modelled. Finally, the Noise-Equivalent Power, NEP_r, the property of the detector defining the noise floor in terms of power ([dBW] or [W]), is modelled from specifications of ExtInGaAs detector sensitivities in technical literature. More details and rationales on the modelling of these losses have been described in *ACCURAID* (2007).

Starting from the transmitted power P_t [dBW], and using all these loss components including the atmospheric attenuation, $L_{atm} = 10 \cdot \log(I_0/I)$ [dB] from the FoMod system (Eq. (3), summing up all extinction components), the OSMod system performs a link-budget computation to obtain the received power, P_r [dBW], and the signal-to-noise density ratio, S/N_0 [dBHz], for LIO signals arriving at the detector. To arrive at S/N_0, first the signal-to-noise ratio (SNR) at the simulated sampling rate f_s, SNR_{fs} [dB], is computed in form of the log-power link budget from P_t to NEP_r:

$$SNR_{fs}\,[\mathrm{dB}] = P_r - NEP_r = (P_t - L_{atm} - L_{tr} - L_{rec} - L_{opt}) - NEP_r \ . \tag{8}$$

Computation of the received power P_r is evidently part of this link budget. Because SNR_{fs} depends on the sampling rate f_S of the measurements, the conversion to S/N_0 has to normalize this SNR_{fs} figure to a unit 1 Hz observational bandwidth,

$$S/N_0\,[\mathrm{dBHz}] = SNR_{fs} + 10 \cdot \log\left(\sqrt{(0.5 \cdot f_S[\mathrm{Hz}])}\right) , \tag{9}$$

where the additional term is the sampling gain, i.e., the SNR gain from downsampling from a sampling rate higher than 2 Hz (equivalent to 1 Hz bandwidth according to Nyquist's theorem) to the 2 Hz sampling rate consistent with the unit bandwidth of 1 Hz.

The S/N_0 ratio, which is an important OSMod output characterizing receiving system performance, allows then straightforward computation of the thermal noise standard error, $\sigma_{I,th}$, for any desired final (potentially down-filtered) sampling rate f_s,

$$\sigma_{I,th}\,[\mathrm{dB}] = 10 \cdot \log\left(1 + \frac{\sqrt{(0.5 \cdot f_S[\mathrm{Hz}])}}{10^{(S/N_0[\mathrm{dBHz}])/10}[\mathrm{W/W}]}\right) . \tag{10}$$

The standard error $\sigma_{I,th}$ profile is used as standard deviation input to a Gaussian white noise generator, which generates a random realization of thermal noise on the modelled intensity profiles consistent with the $\sigma_{I,th}$ profile. This random noise profile is superposed on the received power profile (computed per Eq. (8)), yielding the final simulated intensity profile observable being a key output of the OSMod system to the InRet processing system.

3 Representative LIO Signal Simulation Results

This chapter demonstrates the correct functioning of the enhancements of the EGOPS software made within the scope of the ACCURAID project, which have just been described in the chapter before. Section 3.1 shows LIO ray propagation results generated with the FoMod system, and section 3.2 presents the LIO related output of the OSMod system.

3.1 FoMod Transmission Results

In order to check the proper functioning of FoMod transmission simulations, the FoMod Results were compared with RFM transmission calculations, which were performed on the basis of the same atmospheric models. In particular, the six FASCODE atmospheres for standard, tropical, mid-latitude summer, mid-latitude winter, sub-arctic summer and sub-arctic winter conditions have been used, because these models contain dynamical (temperature, pressure) as well as chemical atmospheric variables (including the six greenhouse gases H_2O, CO_2, CH_4, N_2O, O_3, CO measured by ACCURATE) as a function of height. The main advantages of EGOPS FoMod calculations compared to RFM transmission calculations are that occultation events can be located in a 3D-realistic manner around the Earth, that the ray-tracer in EGOPS is highly accurate also under 3D-variaton of atmospheric fields and that EGOPS accounts for all relevant atmospheric loss effects. RFM, however, uses the assumption of a spherically symmetric vertical-propagation-plane atmosphere and only accounts for molecular absorption. This is why the results of EGOPS and RFM are expected not to be exactly the same, though rather close as to what regards absorption loss (i.e., without defocusing loss) if the absorber of interest dominates extinction at the given frequency.

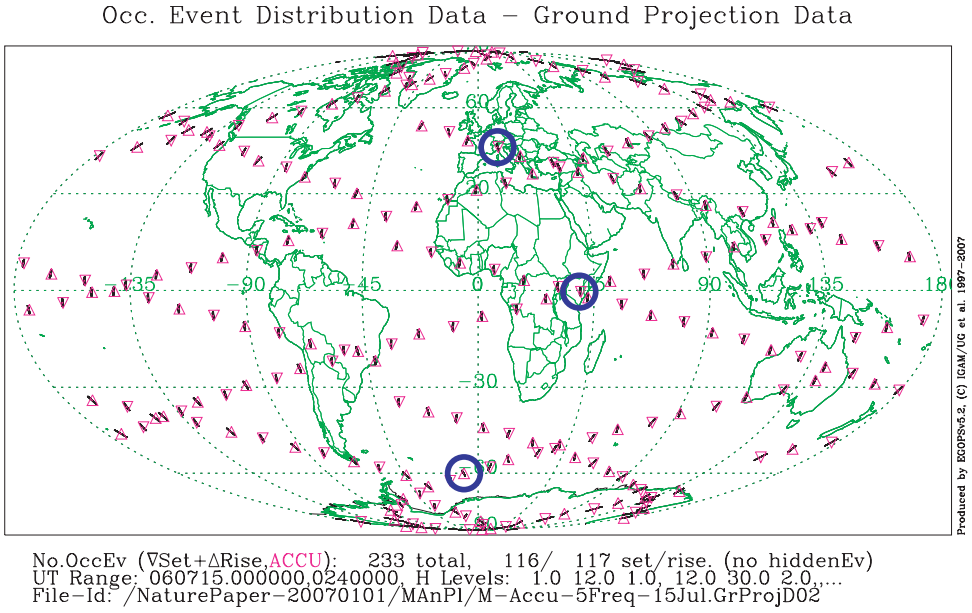

Fig. 3: ACCURATE LIO occultation event locations for July 15, 2006. This MAnPl calculation was based on the ACCURATE satellite geometry (an ACE+ type 2 Tx + 2 Rx constellation; *ESA*, 2004a,b). With this constellation, ~230 occultation events occur per day. The three occultation events encircled by a blue circle are the ones used for the example simulations.

For this report it was decided to present a set of three representative LIO occultation events, which are – in the case of the EGOPS simulations – taking place at different geographic latitudes (see Fig. 3; the needed geometry of the occultation events was computed using the MAnPl system based on satellite orbit data corresponding to the ACCURATE satellite constellation): a standard event located at mid-latitudes, a tropical event, and a sub-arctic winter event, respectively. The tropical and sub-arctic winter event display fairly extreme situations concerning the concentration of water vapour, which is very instructive because this demonstrates a major part of the variation range of LIO transmission signals.

Figures 4 and 5 show transmission results from EGOPS (heavy lines) in comparison to transmission results from RFM (light lines) for the three occultation events selected. Results are shown for all ACCURATE frequencies located at water vapour absorption lines (Fig. 4), at carbon dioxide absorption lines (Fig. 5) as well as at the respective reference channels. The EGOPS results displayed include all atmospheric extinction effects except for defocusing loss. As it can be seen, the results of the two models agree very well. The small differences of up to ~1 dB at 5 km height are due to the additional atmospheric effects in EGOPS (Rayleigh scattering, aerosol extinction, and turbulence/scintillation loss). The defocusing loss – which is not explicitly shown in Figs. 4 and 5 – decreases the transmission as expected from the experience with LRO measurements by up to ~6 dB at a height of 5 km, and by up to ~0.3 dB at 30 km; in between, the influence of defocusing steadily decreases with increasing height.

Concerning the magnitude of the transmission of the different frequencies it can be seen that the ACCURATE signals were properly located in terms of frequency selection. If comparing, for example, the frequencies mainly attenuated by water vapour absorption (Fig. 4) within the different atmospheric conditions (from the very wet tropical atmosphere up to the very dry sub-arctic winter atmosphere), it can be deduced that ACCURATE LIO signals will be able to measure H_2O from 5 to 35 km under all (cloud-free) atmospheric conditions (within clouds it is measured by the LRO signals). This is because the attenuation of the most favourable signal at any given height never exceeds 12 dB or does not drop below 0.5 dB, respectively. Thus the receiver always gets an exploitable signal. This is also valid for all other ACCURATE frequencies. All in all, the EGOPS transmission results are very promising and the comparison with RFM transmission simulations verifies that the EGOPS LIO forward modelling is basically working well.

Figure 6 shows, in the same format as Figure 5, the transmission for the ACCURATE carbon dioxide channels for the three occultation events. The only difference to Figure 5 is that in the EGOPS results in Figure 6 the influence of wind blowing in the line-of-sight direction of the propagating rays was taken into account, too. The wind velocity was extracted from an ECMWF operational analysis of July 15, 2006; the corresponding V_{los} profiles at the three occultation event (tangent point) locations are illustrated in Fig. 7, upper-left panel. As it can be seen, the magnitude of the transmission differs slightly between Figures 5 and 6, whereby the difference is most pronounced in the sub-arctic winter case, where the wind velocity is strongest.

Besides the V_{los} profiles mentioned above, Figure 7 shows the transmission difference between the so-called "wind-1" and "wind-2" line of the ACCURATE frequency set (see *ACCURAID*, 2007, for more details) for windy and motionless atmosphere, respectively, at the three occultation event locations. In the atmosphere at rest ("No wind"), the frequencies of

these channels are nearly lying at the two turning points of the CO_2 absorption line shape, which means that the absorption of the wind-1 and the wind-2 frequency is closely the same in this case because of the symmetry of absorption lines. As Figure 7 shows, the "No wind" case (solid line) confirms this behaviour for heights above about 20 km. If wind is blowing, the CO_2 molecules absorb a slightly different frequency because of the Doppler shift. This causes the difference between the wind-1 and the wind-2 transmission to grow (the stronger the wind, the higher the difference), because one frequency is shifted to higher absorption and the other one to lower absorption across the shape of the absorption line.

Figure 8 further illustrates this behaviour by means of three simple wind conditions: The upper right and the two lower panels show the transmission difference between the two ACCURATE wind lines in three atmospheric conditions (FASCODE standard, tropical, subarctic winter) assuming either constant (dashed and dashed-dotted line) or sinusoidally in height varying (dotted line) wind. The corresponding wind velocities are shown in the upper left panel. Here, wind velocity and direction were assumed to be spherically symmetric; at tangent point, the wind direction equals the ray direction. In order to ensure this simple geometry, a vertical, south-north occultation plane was chosen and wind direction was assumed to be aligned with the occultation plane. For comparison, the case of a motionless atmosphere is illustrated in Fig. 8 as well. Obviously, constant wind velocity leads to a height-dependent transmission difference, largest at about 20 km, where the first derivative of the absorption line is highest. Accordingly, sinusoidally varying wind causes the difference to increase and decrease sinusoidally. Keeping this behaviour in mind, also the shape of the differences shown in Fig. 7 (dashed lines in the respective panels) is well comprehensible.

The wind evidently induces a clearly traceable variation of the difference between the two ACCURATE "wind-1" and "wind-2" transmissions. If this behaviour is adequately exploited in retrieval processing, the line-of-sight wind velocity profile at the tangent point location can be retrieved from ~10-15 to 35-40 km height (cf. *ACCURAID*, 2007). This in turn enables to retrieve the concentration of the absorbing gases with optimal accuracy also in case of strong winds, because the influence of wind can be taken into account in this case.

As it can also be seen from Figs. 7 and 8, below about 20 km the behaviour of the CO_2 absorption line is not exactly symmetric. The turning points of the absorption line drift a little, which is due to the influence of pressure broadening, which increases with decreasing height and causes that a neighbouring CO_2 absorption line, which is located at the wing of the line towards higher wave numbers, gains influence. Since this effect is known, it can be incorporated in the retrieval so that the wind velocity can be retrieved anyhow. Furthermore, the accuracy will decrease with the increase of thermal noise when coming deeper into the upper troposphere, due to the downward increase of measurement noise (see next section 3.2). Influences such as the pressure broadening effects can be well studied using the new EGOPS FoMod capabilities for LIO. EGOPS-based studies will in future contribute to decide whether the currently designated CO_2 line is the most suitable one of all ACCURATE lines for wind retrieval. For example, the $C^{18}OO$ line is a potential alternative.

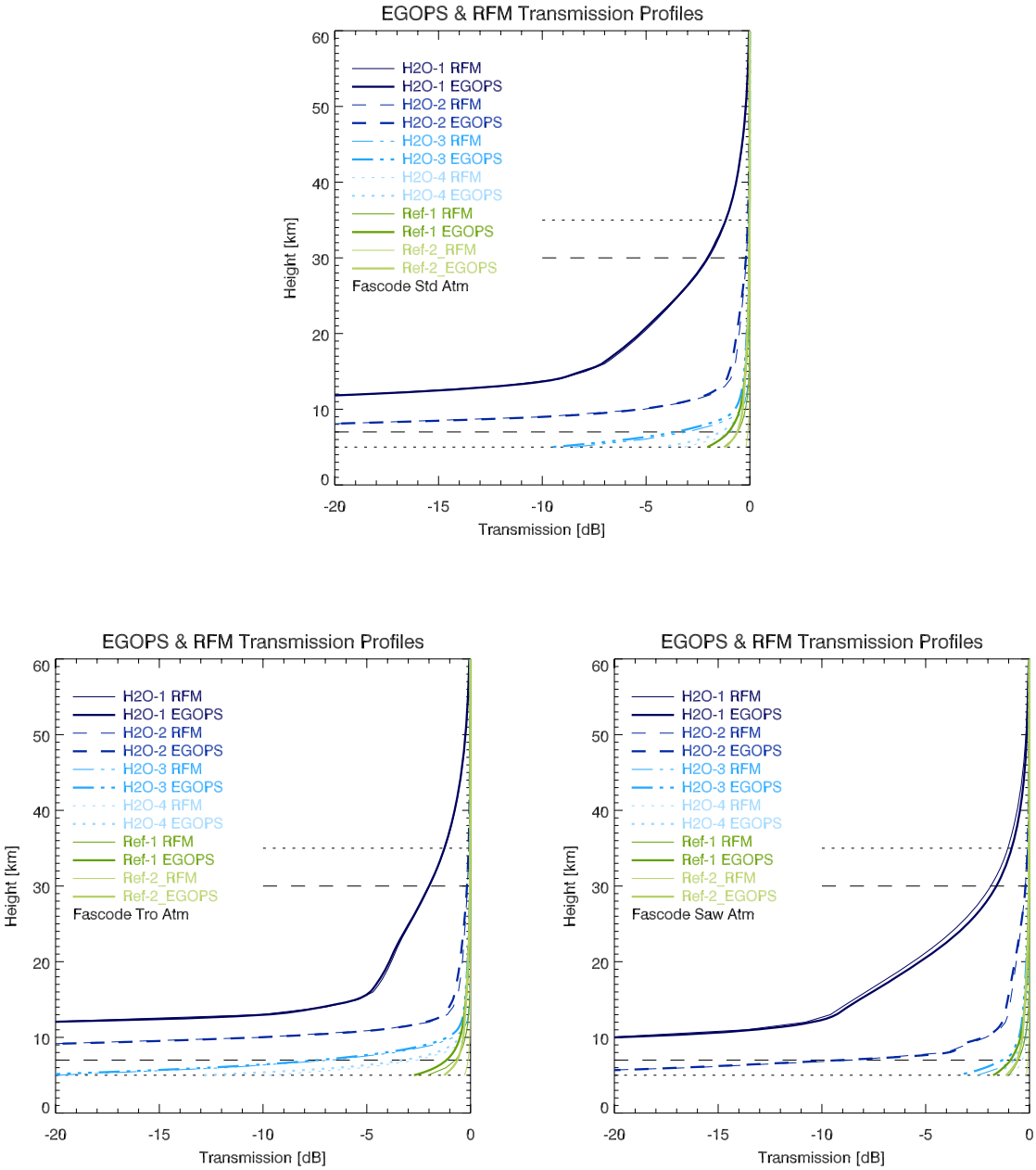

Fig. 4: EGOPS transmission calculations in comparison to RFM transmission calculations for the four ACCURATE water vapour channels (H_2O-1, H_2O-2, H_2O-3, H_2O-4) as well as for two corresponding reference channels (Ref-1, Ref-2; note: the reference channel for the H_2O-2 channel is shown in Fig. 5). Heavy lines denote EGOPS calculations, light lines denote RFM calculations. The upper panel shows the result for FASCODE standard (Std) atmospheric conditions, the lower left panel for tropical (Tro) conditions and the lower right panel for sub-arctic winter (Saw) conditions. The horizontal lines indicate the ACCURATE target (dotted) and threshold (dashed) requirements set for the height range where greenhouse gas profiles shall be provided.

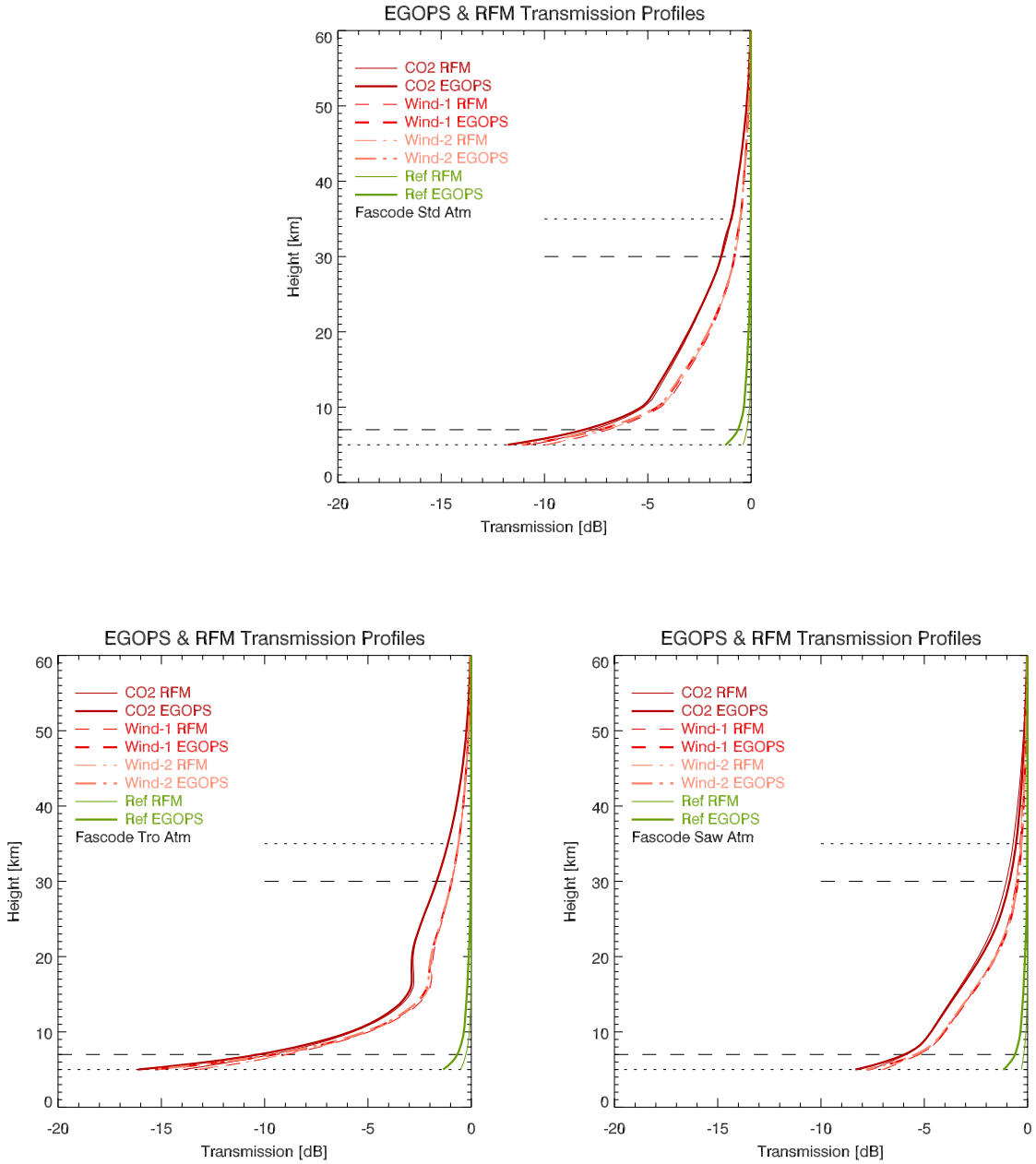

Fig. 5: EGOPS transmission calculations in comparison to RFM transmission calculations for the ACCURATE CO_2, wind-1, wind-2, and the corresponding reference channel (Ref). Heavy lines denote EGOPS calculations, light lines denote RFM calculations. The upper panel shows the result for FASCODE standard (Std) atmospheric conditions, the lower left panel for tropical (Tro) conditions, and the lower right panel for sub-arctic winter (Saw) conditions. The horizontal lines indicate the ACCURATE target (dotted) and threshold (dashed) requirements set for the height range where greenhouse gas profiles shall be provided.

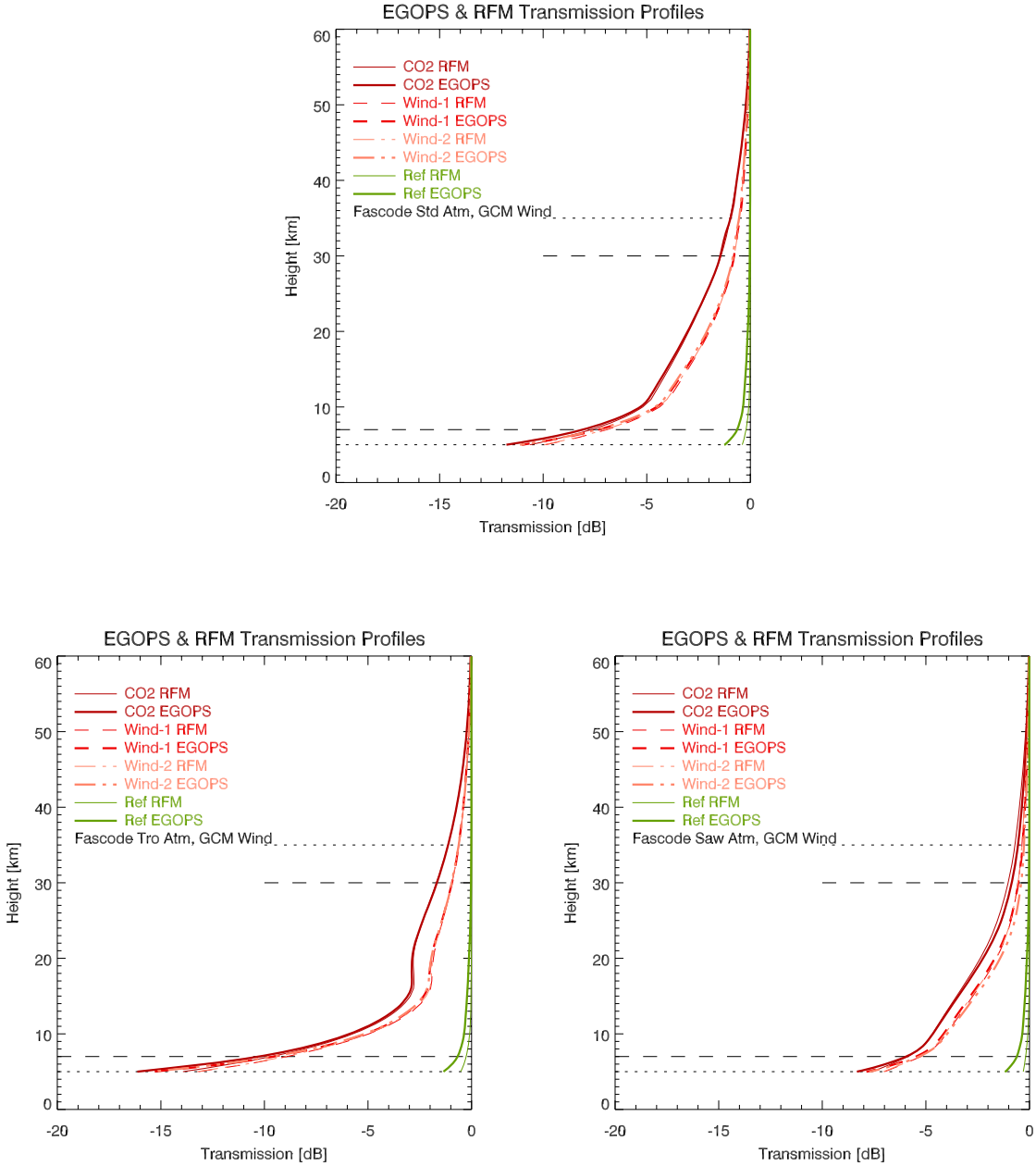

Fig. 6: This figure shows closely the same as Figure 5. The only difference is that in this case a windy atmosphere was adopted. The wind velocity profiles were taken from an ECMWF analysis of July 15, 2006 (illustrated in Fig. 7, upper-left panel).

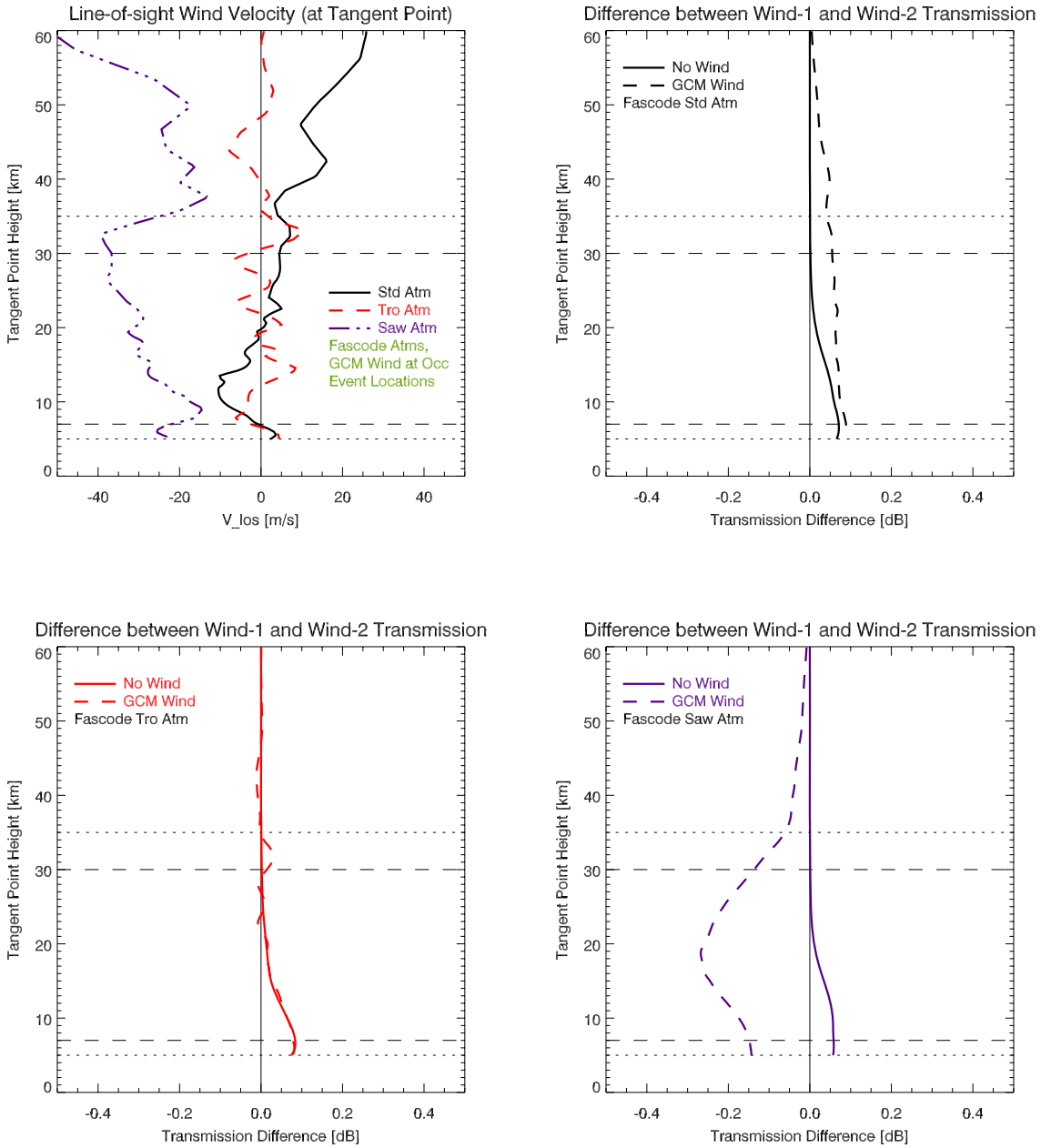

Fig. 7: The upper left panel of this figure shows the line-of-sight wind velocity profiles for the standard (Std), the tropical (Tro) as well as the sub-arctic winter (Saw) occultation event. These wind profiles are underlying the plots of Fig. 6. The other three panels show the transmission difference between the two ACCURATE wind channels (wind-1 minus wind-2) for the standard (Std), tropical (Tro) and sub-arctic winter (Saw) event. The results with GCM wind (dashed line) and without ("No wind", solid line) are shown. The horizontal lines indicate the ACCURATE target (dotted) and threshold (dashed) requirements set for the height range where greenhouse gas profiles shall be provided. Wind profiles shall be provided down to at least 15 km (cf. *ACCURAID*, 2007).

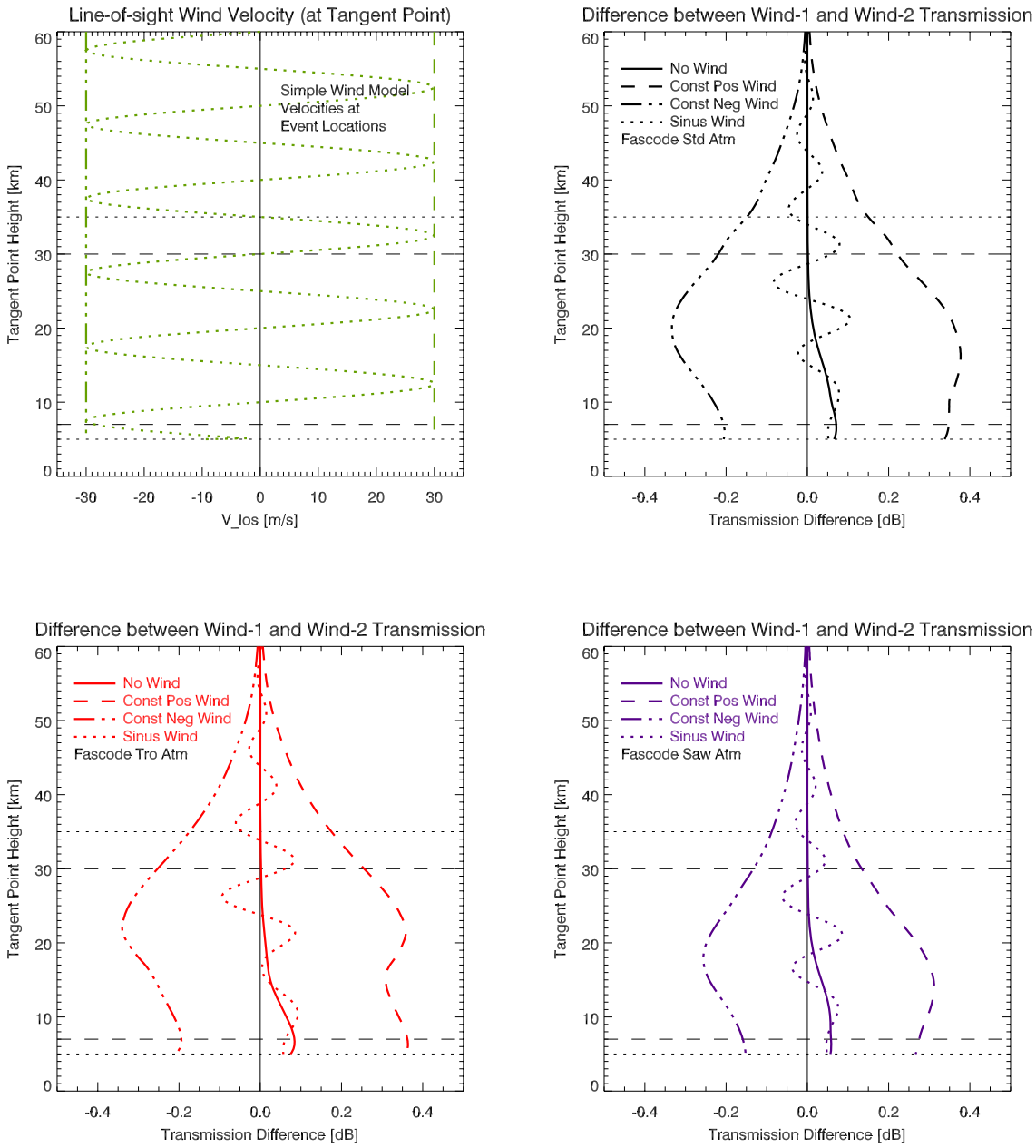

Fig. 8: The upper left panel shows three simple wind conditions, which have been used to compute the differences between the transmissions of the two ACCURATE wind lines (wind-1 minus wind-2) shown in the other panels (dashed line = constant positive wind, dash-dotted line = constant negative wind, dotted line = sinusoidally in height varying wind, solid line = no wind). The results are shown for three different atmospheric conditions: FASCODE standard (Std), tropical (Tro) and sub-arctical winter (Saw) atmosphere. The horizontal lines indicate the ACCURATE target (dotted) and threshold (dashed) requirements set for the height range where greenhouse gas profiles shall be provided. Wind profiles shall be provided down to at least 15 km (cf. *ACCURAID*, 2007).

3.2 OSMod Simulation Results

Within OSMod, instrument-related perturbations of propagating signals are calculated. A main output is the signal-to-noise density ratio S/N_0 (cf. Eqs. (8) and (9)), which is a measure for the quality of the detected signal. Figure 9 representatively shows the S/N_0 ratio for three of the 21 ACCURATE frequencies: the CO_2 signal, the wind-1 signal, and their reference channel signal, respectively. The S/N_0 was computed directly from the FoMod output shown in Fig. 5 and includes estimates of all atmospheric and receiving system perturbations relevant for the ACCURATE LIO technique explained in section 2.2.2. The results shown in this report are representative for all ACCURATE frequencies.

The general behaviour of the S/N_0 meets the expectations. Magnitude and the steady decline of the S/N_0 are adequate and the S/N_0 is higher the smaller the molecular absorption of the signal is (the CO_2 and the wind-1 channel are lying at the centre and at the turning point of a CO_2 absorption line, respectively, and the reference signal is nearly not absorbed). Merely the undulated structure in the upper troposphere region is salient. This effect is due to the defocusing loss modelling as part of the ray-tracing in the FoMod system, where the tropopause structures (with fairly sharp "kinks" in the temperature profile resp. refractivity field) induces these variations. This undulating structure may in future be mitigated by smoother modelling of the tropopause shape in the relatively simple FASCODE atmosphere profiles, which can be achieved by adjustments to the vertical profile interpolation procedure.

Figure 10 displays the influence of the measurement noise of the ACCURATE LIO receiving system modelled as explained along with Eq. (10) in section 2.2.2. In particular, Fig. 10 shows the difference between two received signal intensity profiles, one simulated with including the thermal noise, the other with excluding it ("perfect noise-free reference case"). The level and the general behaviour of the noise meets the expectations deduced from the experience with LRO measurements and IR detector systems, i.e., at high altitudes noise is below the 0.01 dB rms level (i.e., SNR near 30 dB) but it increases to the order of 0.1 dB into the upper troposphere < 10 km where the SNR quite rapidly decreases. Still this intensity accuracy promises fairly good retrieval performance for trace gases, and even winds.

Finally it shall be mentioned that FoMod and OSMod also allow to compute the phase delay of received SWIR signals. This is done with the same algorithms which are already included for phase delay computations of MW and radio signals. Even though the phase delay of SWIR signals is not exploited by the greenhouse gas retrieval (because in reality the phase delay of the short-waved SWIR signals is difficult to measure), the computation of both, LIO and LRO phases enables to investigate the differences in the signal propagation in detail. This is estimated to be very small, because the *Edlen* (Eq. (1)) and *Smith-Weintraub* (Eq. (2)) formulae, which govern the ray propagation, are very similar for the ACCURATE LIO and LRO frequencies. The Smith-Weintraub and the Edlen refractivities differ in dry regions by < 0.1% only; in wet regions by ~7% at 5 km height if the water vapour pressure e amounts to ~2 hPa (frequent case) and by ~15% at 5 km if e amounts to ~4 hPa (more worst case, occurs only in tropics). These differences decrease quickly with increasing altitude and are generally negligible above ~12 km height.

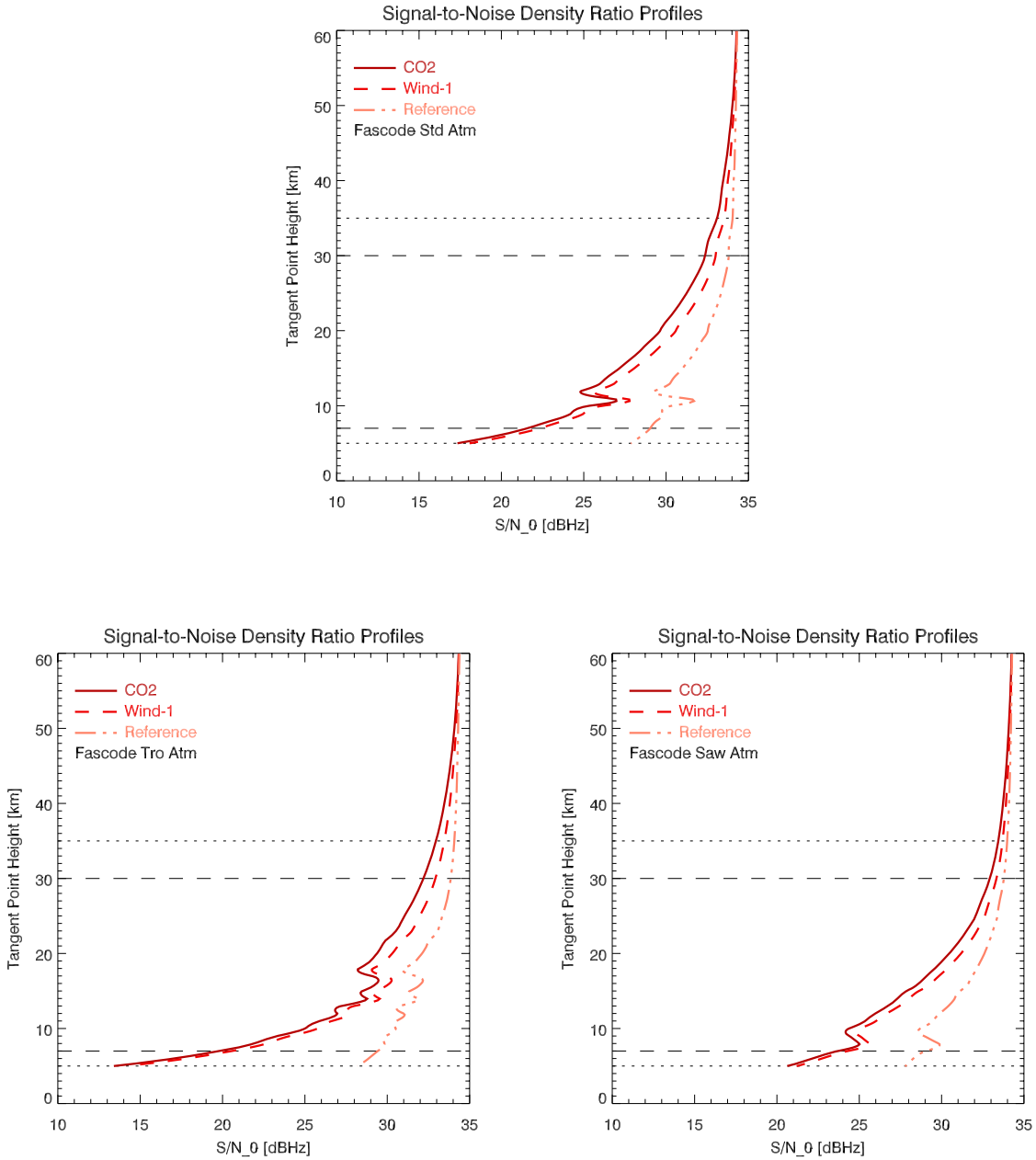

Fig. 9: Signal-to-noise density ratios (S/N_0) for the ACCURATE CO_2, wind-1, and respective reference channel, for the three FASCODE atmospheric conditions (standard - Std, tropical - Tro, sub-arctic winter - Saw). The horizontal lines indicate the ACCURATE target (dotted) and threshold (dashed) requirements set for the height range where greenhouse gas profiles shall be provided.

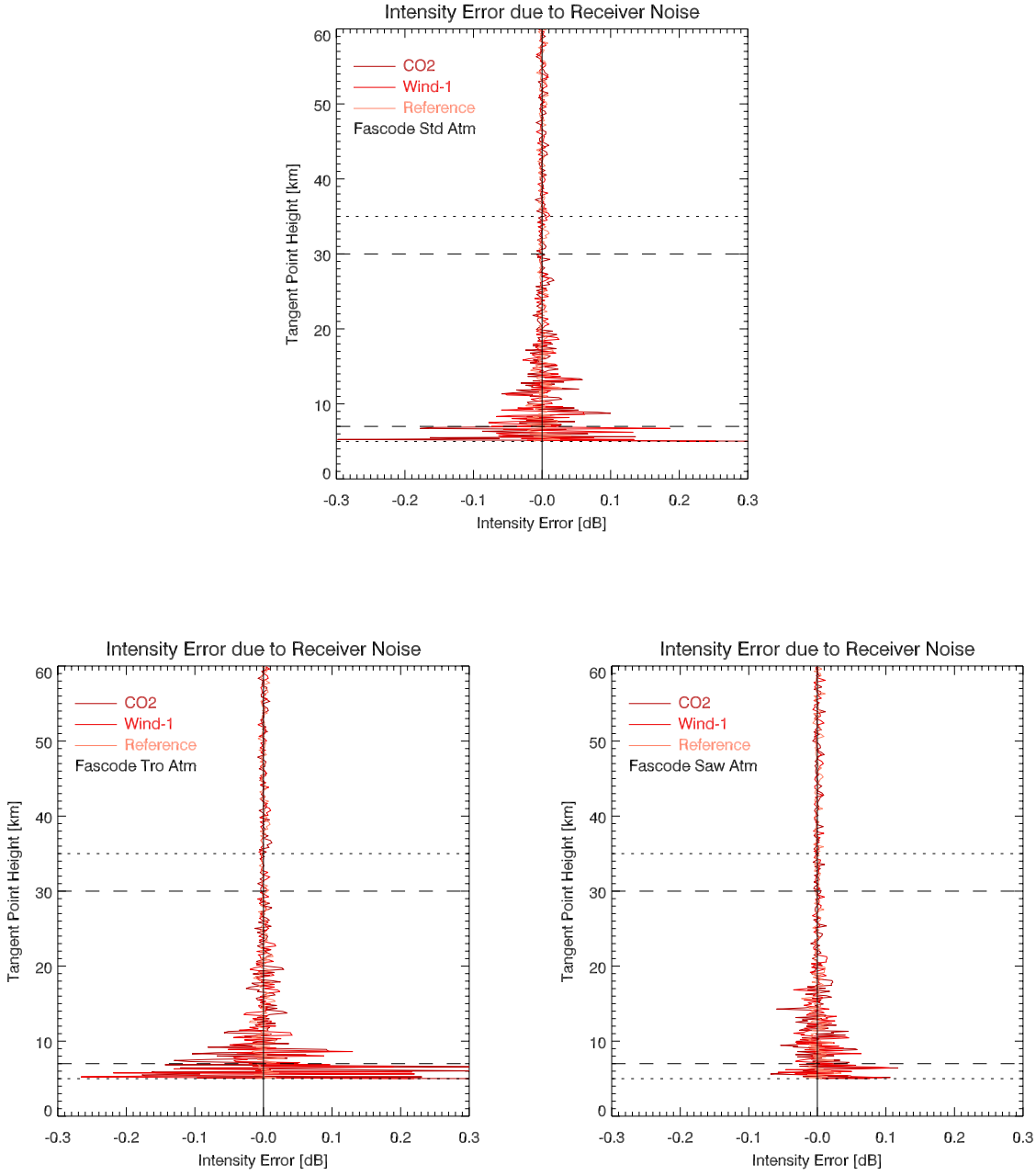

Fig. 10: Error in received intensity (received power) due to receiver noise at a sampling rate of 10 Hz for the ACCURATE CO_2, wind-1, and respective reference channel, respectively. The noise was obtained via computing the difference between a perturbed and an unperturbed intensity and is shown for the FASCODE standard (Std), tropical (Tro), and sub-arctic winter (Saw) atmosphere. The horizontal lines indicate the ACCURATE target (dotted) and threshold (dashed) requirements for the height range where greenhouse gas profiles shall be provided.

(intentionally left blank; back page if double-sided print)

4 Conclusions and Outlook

The results presented in chapter 3 show that the enhancement of EGOPS performed within the scope of the ACCURAID project was successful. The inclusion of the new full atmosphere model as well as the direct integration of the Reference Forward Model (RFM), in order to support the computation of absorption coefficients needed for the forward modelling of ACCURATE LIO measurements, turned out to be effective and efficient. This enabled seamless integration of the SWIR ray tracing signal propagation, including models for atmospheric influences (molecular absorption, Rayleigh scattering, aerosol extinction, turbulence/-scintillation loss) as well as instrument-related influences (propagation loss, reception loss, optical loss, Noise Equivalent Power) on the transmitted SWIR signals.

The results demonstrate that the EGOPS FoMod and OSMod systems can properly handle SWIR frequencies, which is evidenced by comparison of EGOPS FoMod transmission results with RFM transmission results and by inspection of OSMod receiving system modelling results, respectively. The EGOPS system has thus already shown initial utility for ACCURATE mission analyses.

The enhancement of EGOPS for LIO end-to-end simulation, now backed by the encouraging results from the ACCURAID project, will be continued within the scope of the (FFG-ALR) EOPSCLIM project and likely in future ESA studies. In addition, a scheduled ESA-Prodex project will provide important support at EGOPS S/W system engineering level to these future ACCURATE-related enhancements.

A main aim of these follow-on projects is to advance the Inversion/Retrieval system of EGOPS so that full end-to-end simulations of LIO measurements can be performed for studying trace gas and wind retrieval performances in detail. At the moment, a simplified, yet reasonably realistic EGOPS-external performance analysis chain is available, in form of the ALPS (ACCURATE LIO Performance Simulator) system developed in the ACCURAID project, which was used for the performance analyses of ACCURAID WP 3 (*ACCURAID*, 2007). Overall, complementing the EGOPS GRO and LRO end-to-end simulation chains with comparable capabilities for LIO end-to-end simulations provides a further strong boost both to the capabilities of EGOPS itself and to the analysis and promotion of the ACCURATE mission concept on its route towards implementation.

Acknowledgments

The authors gratefully acknowledge all colleagues and their institutions who, in various ways, have supported the preparation of the ACCURATE mission and of this ACCURAID report. M. Gorbunov, V. Sofieva, F. Dalaudier, P. Bernath, R. Hughes, R. Kursinski, and A. Dudhia are particularly acknowledged for their advice. J. Fritzer, J. Ramsauer, M. Schwärz, and H. Krenn (Univ. of Graz) are particularly acknowledged for their contributions and support in course of the initial LIO performance assessments and of the implementation of the EGOPS LIO enhancements, respectively.

The following companies (and colleagues) are acknowledged for advice to the authors on technical aspects during the ACCURAID project:

- TOPTICA Photonics AG (primary advisor A. Deninger); advice on SWIR laser technology and LIO Tx system; www.toptica.com
- Laser Components GmbH (primary advisor J. Kunsch); advice on SWIR detector technology and LIO Rx system; www.lasercomponents.com
- Swedish Space Corporation (primary advisor S. Veldman); advice on preliminary ACCURATE system analysis; www.ssc.se

References

ACCURAID (2007), Kirchengast, G., and S. Schweitzer, ACCURATE LEO-LEO Infrared Laser Occultation Initial Assessment: Requirements, Payload Characteristics, Scientific Performance Analysis, and Breadboarding Specifications, *Tech. Rep. for FFG-ALR No. 3/2007*, 56 pp, Wegener Center, Univ. of Graz, Austria.

ACCURATE (2005), ACCURATE — Atmospheric Climate and Chemistry in the UTLS Region and climate Trends Explorer, *ESA Earth Explorer Core Mission Proposal/Ref.No. CCM2-13*, 19 pp, International Responding Team & WegCenter/UniGraz, Graz, Austria.

Anderson, G.P., S.A. Clough, F.X. Kneizys, J.H. Chetwynd, and E.P. Shettle (1986), AFGL atmospheric constituent profiles (0–120 km), *Tech. Rep. TR-86-0110*, AFGL.

Edlen, B., The refractive index of air, *Metrologia 2*, 71–80, 1966.

ESA (2004a), ACE+ — Atmosphere and Climate Explorer (4th report of Reports for Mission Selection, The Six Candidate Earth Explorer Missions), *ESA Spec. Publ. SP-1279(4)*, 60 pp, ESA/ESTEC, Noordwijk, NL.

ESA (2004b), ACE+ — Atmosphere and Climate Explorer Technical and Programmatic Annex (annex to 4th report of Reports for Mission Selection, The Six Candidate Earth Explorer Missions), *ESA Spec. Publ. SP-1279(4) Annex*, 39 pp, ESA/ESTEC, Noordwijk, NL.

ESA (2005), Call for Ideas for the Next Earth Explorer Core Missions, *Doc.No. ESA/EXPLORER/CCM-02*, 19 pp (incl. Annexes), ESA, March 2005.

ESA (2006), The Second Call for Earth Explorer Core Mission Ideas: The Evaluation of the Twenty-Four Proposals *plus Annex Individual Assessment Reports of Mission Proposals, including* ACCURATE – Atmospheric Climate and Chemistry in the UTLS Region And climate Trends Explorer (CCM-13), *Doc.No. ESAC/Apr.06*, 16 pp + Annex pp 65-69, ESA, April 2006.

HITRAN (2007), http://cfa-www.harvard.edu/HITRAN, Internet, Feb. 2007.

Kirchengast, G., J.M. Fritzer, M. Schwaerz, S. Schweitzer, and L. Kornblueh (2004a), The Atmosphere and Climate Explorer Mission ACE+: Scientific Algorithms and Performance Overview. *Tech. Rep. for ESA/ESTEC No. 2/2004*, IGAM, Univ. of Graz, Austria. [on-line: www.wegcenter.at > Research > ARSCliSys > Publications]

Kirchengast, G., S. Schweitzer, J. Ramsauer, and J. Fritzer (2004b), End-to-end Generic Occultation Performance Simulator Version 5 (EGOPS5) Software User Manual (Overview-, Reference-, and File Format Manual), *Tech. Rep. for ESA/ESTEC No. 6/2004*, Inst. for Geophys., Astrophys., and Meteorol., Univ. of Graz, Austria. [on-line: www.wegcenter.at > Research > ARSCliSys > Publications]

Kirchengast, G., S. Schweitzer, J. Ramsauer, and J. Fritzer (2007), EGOPSv52 Software User Manual (Overview, Reference, and File Format Manual), *Tech. Rep. for ESA/ESTEC No. 4/2007*, Wegener Center & Inst. for Geophys., Astrophys., and Meteorol., Univ. of Graz, Austria.

Kursinski, E.R., G.A. Hajj, J.T. Schofield, R.P. Linfield and K.R. Hardy (1997), Observing Earth's atmosphere with radio occultation measurements using the Global Positioning System, *J. Geophys. Res., 102,* 23,429–23,465.

Kursinski, E.R., S. Syndergaard, D. Flittner, D. Feng, G. Hajj, B. Herman, D. Ward, and T. Yunck (2002), A microwave occultation observing system optimized to characterize atmospheric water, temperature and geopotential via absorption, *J. Atmos. Oceanic Technol., 19(12)*, 1897–1914.

Liou, K.N. (2002), Introduction to Atmospheric Radiation, 2nd edition, *Academic Press*, *Elsevier Science*, California, USA. ISBN: 0-12-451451-0

NOAA (2005), Pinatubo effects in the Arctic as derived from Airborne and Surface observations, *NOAA ESRL Global Monitoring Division*, on-line report at: www.cmdl.noaa.gov/star/ agasp2.html (Internet, Feb. 2007)

OPAC (2004a), Kirchengast, G., Occultations for Probing Atmosphere and Climate: Setting the Scene, in *Occultations for Probing Atmosphere and Climate,* Kirchengast-Foelsche-Steiner (eds.), 1–8, Springer, Berlin-Heidelberg. [on-line: www.wegcenter.at > Research > ARSCliSys > Publications]

OPAC (2004b), Kirchengast, G., and P. Hoeg, The ACE+ Mission: An Atmosphere and Climate Explorer based on GPS, GALILEO, and LEO-LEO Radio Occultation, in *Occultations for Probing Atmosphere and Climate,* Kirchengast-Foelsche-Steiner (eds.), 201–220, Springer, Berlin-Heidelberg. [on-line: www.wegcenter.at > Research > ARSCliSys > Publications]

RFM (1996), High Level Algorithm Definition Document, *Rep. for ESA/ESTEC*, *Contract No.11886/96/NL/GS*, Institute of Atmospheric, Oceanic and Planetary Physics, Oxford University, United Kingdom.

RFM (2007), http://www-atm.physics.ox.ac.uk/RFM/, Internet, Feb. 2007.

Rothman, L.S., et al. (2005), The HITRAN 2004 Molecular Spectroscopic Database, *J. Quant. Spectroscopy and Rad. Transfer*, *96*, 139-204.

Russell, P.B., J.M. Livingston, R.F. Pueschel, J.J. Bauman, J.B. Pollack, S.L. Brooks, P. Hamill, L.W. Thomason, L.L. Stowe, T. Deshler, E.G. Dutton, and R.W. Bergstrom (1996), Global to microscale evolution of the Pinatubo volcanic aerosol derived from diverse measurements and analyses, *J. Geophys. Res., 101,* 18,745–18,764.

Salby, M.L. (1996), *Fundamentals of Atmospheric Physics,* Academic Press, San Diego, Calif.

Smith, E.K., and S. Weintraub (1953), The constants in the equation for atmospheric refractive index at radio frequencies, *Proc. of the IRE*, *41*, 1035–1037.

Thomason, L.W., and G. Taha (2003), SAGE III aerosol extinction measurements: Initial results, *Geophys. Res. Lett., 30,* 1631, doi:10.1029/2003GL017317.

– end of document –